

## Nuclear magnetic resonance of $^{14}\text{N}$ and $^{35}\text{Cl}$ in ammonium perchlorate

This article has been downloaded from IOPscience. Please scroll down to see the full text article.

1989 J. Phys.: Condens. Matter 1 4649

(<http://iopscience.iop.org/0953-8984/1/28/014>)

View [the table of contents for this issue](#), or go to the [journal homepage](#) for more

Download details:

IP Address: 171.66.16.93

The article was downloaded on 10/05/2010 at 18:28

Please note that [terms and conditions apply](#).

## Nuclear magnetic resonance of $^{14}\text{N}$ and $^{35}\text{Cl}$ in ammonium perchlorate

T J Bastow and S N Stuart

Division of Materials Science and Technology, CSIRO Australia, Locked Bag 33,  
Clayton, Victoria 3168, Australia

Received 9 January 1989

**Abstract.** The nuclear quadrupole interaction tensor of  $^{14}\text{N}$  and  $^{35}\text{Cl}$  and the diamagnetic shielding tensor of  $^{35}\text{Cl}$  in ammonium perchlorate at room temperature have been determined from nuclear magnetic resonance rotation studies of single crystals.

### 1. Introduction

There has been some debate over the possible existence of phase transitions in ammonium perchlorate,  $\text{NH}_4\text{ClO}_4$ , at low temperatures [1–5]. Since NMR can be a sensitive probe of local order and dynamics at structural transitions, a number of NMR investigations of this question have been made, using  $^1\text{H}$  as the probe nucleus in powder specimens. (See references cited in [3].) Recently the scope of these investigations has been extended in a  $^{35}\text{Cl}$  and  $^2\text{H}$  study of  $T_1$  over the temperature range 150–300 K [4], and subsequently by a  $^{35}\text{Cl}$  single-crystal study over the range 4–300 K [5]. Nevertheless, a full description of the nuclear electric field gradient (EFG) and chemical shielding in this material at any temperature has been lacking.

In order to establish a benchmark for future work, we have made single-crystal rotation studies at 296 K of both the normal hydrogenous and the fully deuterated compound. The following nuclear tensor properties have been completely determined with respect to crystal axes:

- (i) quadrupole interaction at the  $^{14}\text{N}$  site (in  $\text{NH}_4\text{ClO}_4$  and  $\text{ND}_4\text{ClO}_4$ ) and the  $^{35}\text{Cl}$  site (in  $\text{NH}_4\text{ClO}_4$ );
- (ii) diamagnetic shielding at the  $^{35}\text{Cl}$  site in  $\text{NH}_4\text{ClO}_4$ .

We have further investigated the possibility [2] of a phase transition occurring near 180 K in  $\text{NH}_4\text{ClO}_4$  by examining the temperature dependence of the  $^{14}\text{N}$  quadrupole coupling over the range 150 K to 296 K.

The crystal structure of ammonium perchlorate at room temperature has been reported as orthorhombic ( $Z = 4$ ) with space group  $Pnma$  [1–6]. A significant feature of this assignment is that the crystallographic ( $ac$ ) plane containing the nitrogen and chlorine atoms is a mirror plane, so that the  $b$  axis of the crystal should be a principal axis of both nuclear EFG and nuclear shielding. This means that one rotation about the  $b$  axis is sufficient to determine the quadrupole interaction tensor [7]. Rotations about two axes are necessary to determine the shielding tensor, which is not traceless.

## 2. Experimental procedure

Crystals of the hydrogenous material were grown from aqueous solution at room temperature. Deuterated crystals were grown in heavy water, using starting material prepared by repeated evaporation from heavy water (99.5% enriched): the eventual level of deuteration is estimated to be greater than 99%.

All the crystals used in this work were of the lozenge form noted in [1] and were bounded by parallelogram {001} faces and rectangular {210} faces. We also noticed during our crystal growing a chisel-ended columnar form with the same faces and (120) axis. Our orientation assignment was verified in both cases by optical goniometry and also by x-rays with an independent single-crystal orientation on a four-circle goniometer, using the published structural data [1]. We chose the lozenge form for the measurements reported here because it was easier to orient in our rotation stage.

The spectrometer used was a Bruker MSL 400 operating in a nominal field of 9.4 T. Direct  $^{35}\text{Cl}$  and  $^{14}\text{N}$  spectra were obtained by Fourier transforming the free induction decay following the solid echo pulse sequence:  $(\frac{1}{2}\pi)_x-t-(\frac{1}{2}\pi)_y-t-aq$ . Values of  $t$  were 30  $\mu\text{s}$  for  $^{35}\text{Cl}$  and 40  $\mu\text{s}$  for  $^{14}\text{N}$ . The  $\frac{1}{2}\pi$  pulse widths were approximately 4  $\mu\text{s}$  for both nuclei.

For  $^{14}\text{N}$ , preliminary estimates of quadrupole coupling parameters were taken from powder spectra, which yielded

$$e^2qQ/h = 53.3 \text{ kHz}, \eta = 0.13 \text{ for } \text{NH}_4\text{ClO}_4 \text{ and}$$

$$e^2qQ/h = 52.2 \text{ kHz}, \eta = 0.11 \text{ for } \text{ND}_4\text{ClO}_4.$$

These values accurately foreshadowed those obtained subsequently from the single-crystal measurements.

Single-crystal rotation patterns were derived from spectra recorded at a temperature of 295.7(3) K. The specimen was mounted with one of its crystallographic axes parallel to the rotation axis which was in turn perpendicular to the field. Free induction decays for the  $\pm(I, I-1)$  transitions of  $^2\text{H}$  and  $^{14}\text{N}$  ( $I=1$ ) and  $^{35}\text{Cl}$  ( $I=\frac{3}{2}$ ) were recorded every  $15^\circ$  over a full circle and, separately for the  $(\frac{1}{2}, -\frac{1}{2})$  transition of  $^{35}\text{Cl}$ , at  $7.5^\circ$  intervals over a half circle. Typical line-widths (FWHM) for the  $^{14}\text{N}$  resonances were 0.25 kHz in  $\text{NH}_4\text{ClO}_4$  and 0.2 kHz in  $\text{ND}_4\text{ClO}_4$ ; the line-width for  $^{35}\text{Cl}$  was around 0.9 kHz for the satellite transitions and varied (with angle) between 0.3 and 1.0 kHz for the central transition. Resonance frequencies were observed during rotations about all three crystal axes, for reasons of completeness. The  $^2\text{H}$  spectra are described below (§ 6).

We also measured the  $^{14}\text{N}$  quadrupolar splittings in a single crystal of  $\text{NH}_4\text{ClO}_4$  as a function of temperature between 296 and 150 K, at two different angular settings,  $\angle(b, B) = 90^\circ$ ,  $\angle(a, B) = 10^\circ, 45^\circ$  (chosen rather arbitrarily). As an example, figure 3(a) and 3(b), discussed in § 3.3, shows the temperature dependence at  $\angle(a, B) = 45^\circ$  of the two splittings that were seen.

The frequency reference for  $^{14}\text{N}$  and  $^{35}\text{Cl}$  is taken from solid ammonium chloride. (The Larmor frequencies are 28.913 and 39.207 MHz, respectively.)

## 3. Quadrupolar splitting

The resonances were paired by a graphical assignment and their frequency separations studied as functions of angle. Figures 1 and 2 show the resulting rotation patterns with the  $b$  axis perpendicular to the field.

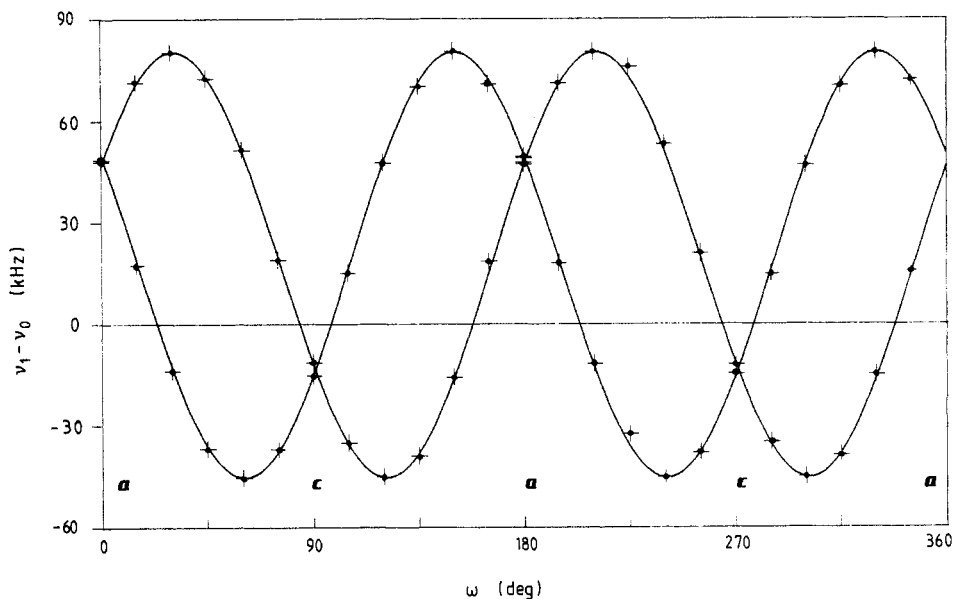


**Figure 1.** NMR rotation pattern of  $^{14}\text{N}$  splitting in a single crystal of  $\text{NH}_4\text{ClO}_4$ : rotation axis  $b$  normal to field  $B$ , angle  $\omega = 0$  when  $a \parallel B$ . +, measured splittings; the curves are calculated using the parameters of table 4(a) and an angular offset of  $0.95^\circ$ .

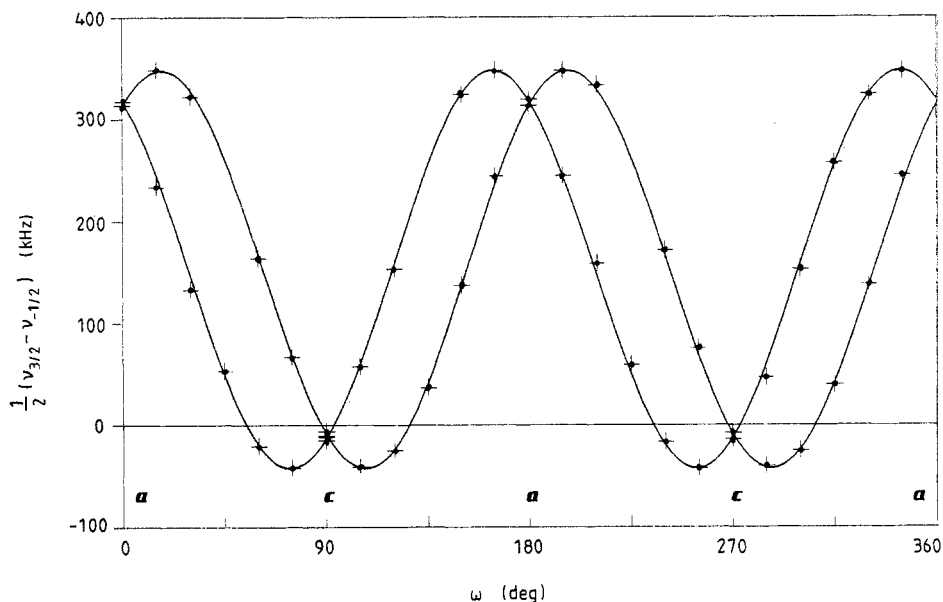


**Figure 2.** NMR rotation pattern of half the satellite separation of  $^{35}\text{Cl}$  in a single crystal of  $\text{NH}_4\text{ClO}_4$ , for the same rotation as in figure 1. +, measured values; curves are calculated using the parameters of table 4(b) and an angular offset of  $0.71^\circ$ .

It is clear from figures 1 and 2 that the rotation about the  $b$  axis shows first-order quadrupolar splitting from two sites which differ only in their opposite orientation with respect to  $a$  (or  $c$ ); in rotation about the  $a$  or  $c$  axis (not reproduced here), the two

splittings remain practically coincident. This is consistent with the point group symmetry of the structure,  $mmm$  with  $Z = 4$ , in which there are two magnetically inequivalent molecules. For both N and Cl, one of the principal axes, located where the splitting is stationary, lies along the  $b$  axis of the crystal. This is just as required by the site symmetry of reflexion in the  $(ac)$  plane.

### 3.1. Numerical method

The observed splittings have been fitted with sinusoidal functions of angle by a method of extended least squares. The ordinary method of varying the linear parameters to minimise the frequency residual sum of squares has one shortcoming. The frequency determination is much less accurate at the inflexion of a curve than at the turning-point, because of angular uncertainty, and so a bias is introduced into estimates of parameters. Therefore, we have chosen to vary the angles from their nominal (observed) value in such a way that the overall frequency residual is minimised with respect to parameters and angles at the same time. The condition of stationarity is a trigonometric, not a linear, one, and it is solved iteratively by Newton's method, using a curvature matrix which typically is of order 24. The problem is that this matrix is not positive definite, and we are obliged to compute its positive partial inverse (typically of rank 22), after decomposing it into its principal idempotents. The result is a set of adjusted angles, whose deviation from the starting set is about  $1.0^\circ$  in RMS, a minimal value which can be taken as the standard deviation of our angular setting. (Note that the method does not require prior estimation of this quantity.) Generally we find that this produces a much improved fit to the observed frequencies.

### 3.2. Data analysis

The frequency separation between transitions  $(m, m - 1)$  and  $(1 - m, -m)$ , where  $m = I$  for each nucleus, can be related to the component of a symmetric tensor  $\nu_Q$  expressed in the laboratory frame ( $Oxyz$ ,  $Oz \parallel B$ ):

$$\nu_m - \nu_{1-m} = (2m - 1)(\nu_Q)_{zz}. \quad (1)$$

The tensor  $\nu_Q$  may be called the *quadrupole frequency tensor* because, when third and higher order terms are negligible, its primary eigenvalue is the quadrupole frequency (conventionally designated  $\nu_Q$ ), such that  $e^2qQ/h = \frac{2}{3}I(2I - 1)\nu_Q$ .

The tensor is then transformed to a cartesian frame (with axes 1 2 3) fixed in the crystal and coinciding with the respective crystallographic axes ( $a b c$ ), in the manner described in [7]. The angular origin ( $\omega_0$ ) of each rotation has been adjusted slightly to conform with the point group symmetry, corresponding to the case (1) adjustment of Volkoff *et al* [7]. The results are given in tables 1 and 2. Although standard errors obtained from the least-squares fit suggest that different rotations may be of different accuracy, this is probably not very significant; in compounding the full tensor from the separate rotations, therefore, the components are weighted equally. The error given in the composite column is that based on either internal or external consistency, whichever is the greater, as recommended in [8]. The components  $(\nu_Q)_{zz}$ , calculated using the mean

**Table 1.**  $^{14}\text{N}$  quadrupole frequency tensor (in kHz), components with respect to crystal axes 1 2 3; offset angles  $\omega_0$ .

Rotation axis $\omega_0$ (deg)	$\text{NH}_4\text{ClO}_4$			$\text{ND}_4\text{ClO}_4$	
	<i>a</i>	<i>b</i>	<i>c</i>	Composite	<i>b</i>
	1.17	0.95	2.67		-0.51
11	48.424(23)	48.423(20)	48.522(7)	48.456(33)	47.466(25)
22	-35.009(20)	-35.038(23)	-34.960(7)	-35.002(23)	-34.444(32)
33	-13.415(20)	-13.385(20)	-13.562(9)	-13.454(55)	-13.022(25)
12	—	—	0.000(6)	0.000(6)	—
31	—	$\pm 54.699(16)$	—	$\pm 54.699(16)$	$\pm 53.634(23)$
23	0.000(16)	—	—	0.000(16)	—

**Table 2.**  $^{35}\text{Cl}$  quadrupole frequency tensor (in kHz), components with respect to crystal axes 1 2 3, for  $\text{NH}_4\text{ClO}_4$ ; offset angles  $\omega_0$ .

Rotation axis $\omega_0$ (deg)	<i>a</i>	<i>b</i>	<i>c</i>	Composite
		-0.86	0.71	0.97
11	315.25(6)	315.77(21)	316.10(7)	315.71(25)
22	-304.37(5)	-304.81(26)	-305.61(7)	-304.93(36)
33	-10.87(5)	-10.96(21)	-10.49(8)	-10.77(14)
12	—	—	0.00(6)	0.00(6)
31	—	$\pm 106.67(20)$	—	$\pm 106.67(20)$
23	0.00(4)	—	—	0.00(4)

values of tables 1 and 2 with the appropriate angular offset, are compared with the observed splittings in figures 1 and 2. After principal axis transformation, the quadrupole coupling parameters are collected in table 4. The coupling constant for  $^{35}\text{Cl}$  is seen to be somewhat greater than the 600 kHz estimated in [5].

### 3.3. Temperature variation

Within the accuracy of our measurements, the  $^{14}\text{N}$  splittings at each setting have been found to vary smoothly with temperature. From the data at  $\angle(a, B) = 45^\circ$  (figure 3(a) and (b)) and similar data for  $\angle(a, B) = \omega_0 + 10^\circ$  (not shown), and with the assumption of invariant point group symmetry, it is possible to derive the components of the quadrupole frequency tensor at each temperature. Figure 3(c) shows the temperature dependence of the derived coupling constant, the uncertainty of which is of order 1.3 kHz. The asymmetry is poorly determined but appears not to exceed its room-temperature value down to 150 K. The orientation of the tensor appears to be constant over this range.

## 4. Diamagnetic shielding

The isotropic chemical shift of  $^{14}\text{N}$  in  $\text{NH}_4\text{ClO}_4$  has been determined by averaging the mean resonant frequency over all three rotations, since the second-order quadrupolar

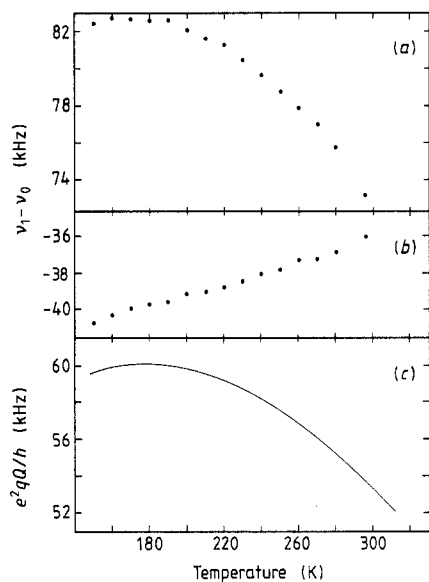


**Figure 3.** Temperature dependence of (a) the outer and (b) the inner quadrupolar splittings of  $^{14}\text{N}$  in  $\text{NH}_4\text{ClO}_4$  with the field oriented along cartesian (1 0 1); (c) inferred quadrupole coupling constant of  $^{14}\text{N}$ .

shift can be shown to be negligible in the mean. The shielding is 18.4(8) PPM with respect to  $^{14}\text{NH}_4\text{Cl}$ . The mean frequency over the  $b$  rotation is lower by 22(9) Hz in the deuterated compound, showing an isotope shift of 0.8(3) PPM; this is comparable with 1.171 PPM found in aqueous solution [9].

The central ( $\frac{1}{2} - \frac{1}{2}$ ) transition frequency  $\nu_{1/2}$  of  $^{35}\text{Cl}$  (figure 4) has been analysed in terms of first-order chemical shift and second-order quadrupolar shift, which have different angular behaviour:

$$\nu_{1/2} = (1 - \sigma_{zz})\nu_L + \nu_{1/2}^{(2)}. \quad (2)$$

In the first-order term  $\sigma_{zz}$  is the component of shielding expressed in the laboratory frame, relative to the reference Larmor frequency  $\nu_L$ . The second-order shift can be calculated from the quadrupole frequency tensor  $\nu_Q$ , determined above, when it is expressed in the laboratory frame [10]:

$$\nu_{1/2}^{(2)} = -\{2(\nu_Q)_{xz}^2 + 2(\nu_Q)_{yz}^2 - (\nu_Q)_{xy}^2 - \frac{1}{4}[(\nu_Q)_{xx} - (\nu_Q)_{yy}]^2\}/3\nu_L. \quad (3)$$

With an offset angle ( $\omega_0$ ) chosen by trial and error, the second-order shifts have been calculated from equation (3) and subtracted from the observed frequencies, and the remainder fitted to sinusoids by ordinary least squares (that is, not varying angles). The components of the resulting shielding tensor are shown in table 3, the composite tensor with its errors being calculated as before. (Note that only the symmetric part of the shielding tensor can be measured here.) Frequencies calculated from the composite tensor with the appropriate angular offset are compared with experiment in figure 4. Results of principal axis transformation are included in table 4(b). No corrections have been made for bulk diamagnetism and crystal shape.

The  $^{35}\text{Cl}$  isotropic shielding,  $\sigma_0 = \frac{1}{3} \text{tr } \sigma = -917.5(7)$  PPM, is not significantly different from that of a small sharp line which we attribute to entrapped liquid; and it may be compared with  $-930$  PPM estimated from a powder specimen [4]. The shielding anisotropy ( $\Delta\sigma$ ), however, not only exhibits the expected site symmetry but, as can be seen by comparing tables 2 and 3, is geometrically similar to the EFG tensor.

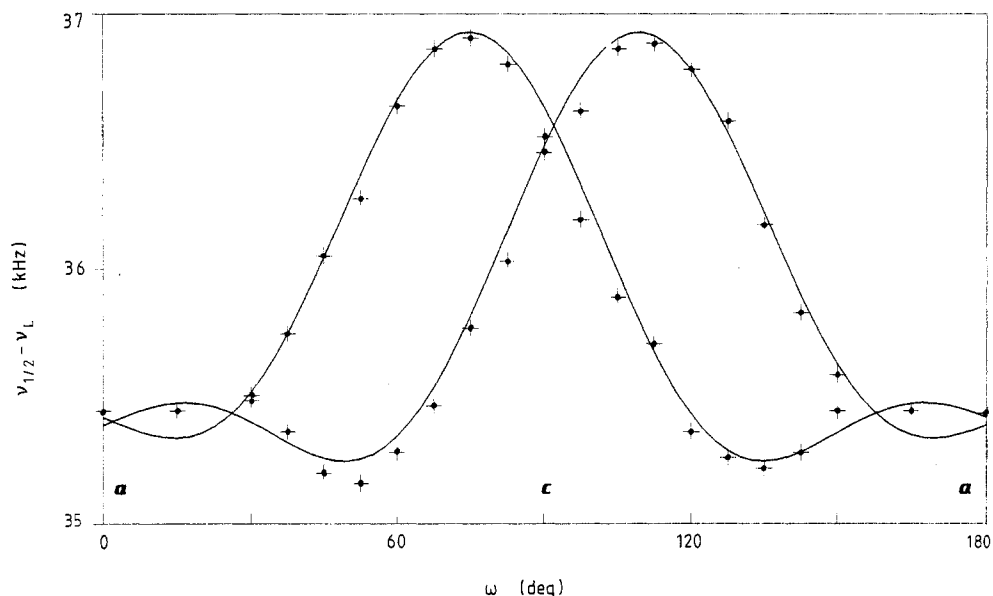


**Figure 4.** NMR rotation pattern for central transition of  $^{35}\text{Cl}$  in a single crystal of  $\text{NH}_4\text{ClO}_4$ , for the same rotation as in figure 1. +, observations; the curves show frequencies calculated from equations (2) and (3) using the parameters of table 4(b) and an angular offset of  $2^\circ$ .

**Table 3.**  $^{35}\text{Cl}$  shielding tensor (in kHz), components with respect to crystal axes 1 2 3, for  $\text{NH}_4\text{ClO}_4$ ; offset angles  $\omega_0$ .

Rotation axis $\omega_0$ (deg)	<i>a</i>	<i>b</i>	<i>c</i>	Composite
	0	2	2	
11	—	35.453(14)	35.368(15)	35.411(43)
22	36.601(7)	—	36.546(15)	36.574(28)
33	36.011(7)	35.865(14)	—	35.938(73)
12	—	—	0.040(14)	0.000(42)
31	—	$\pm 0.235(12)$	—	$\pm 0.235(12)$
23	0.000(6)	—	—	0.000(6)

## 5. Crystal field calculation

Our observations of non-zero quadrupole coupling and shielding anisotropy confirm that both the ammonium and the perchlorate groups are distorted from regular tetrahedral symmetry. Such distortion is likely to be related to the crystal field that acts on each molecular ion. It is desirable to estimate this field, which may suggest a molecular assignment of the nuclear interaction tensors. The field acting on either group can roughly be modelled by point charges of  $(+e)$  at N and  $(-e)$  at Cl; we have computed the resulting local electric field at the N and Cl sites, using our program EFG5 and taking the positional parameters from [6].

The field acting on the  $\text{NH}_4$  group amounts to  $0.083 \text{ V \AA}^{-1}$ , and its cartesian direction is  $(-0.897 \ 0 \ 0.443)$  in the *ac* plane shown in figure 1 of [1]. This direction is  $4^\circ$  from one



**Table 4.** Nuclear interaction tensors (a) for  $^{14}\text{N}$ , and (b) for  $^{35}\text{Cl}$ , in ammonium perchlorate at 295.7(3) K. Quadrupole coupling constant  $e^2qQ/h$ , and asymmetry parameter  $\eta$ ; isotropic diamagnetic shielding  $\sigma_0$  (from solid  $\text{NH}_4^{35}\text{Cl}$ ); eigenvalues of shielding anisotropy  $\Delta\sigma_X$ ,  $\Delta\sigma_Y$ ,  $\Delta\sigma_Z$ ; angles between principal axes  $X$ ,  $Y$ ,  $Z$  and crystal axes  $a$ ,  $b$ ,  $c$ .

(a)	$^{14}\text{NH}_4\text{ClO}_4$	$^{14}\text{ND}_4\text{ClO}_4$		
$ e^2qQ/h $ (kHz)	53.568(20)	52.530(16)		
$\eta$	0.1288(6)	0.1257(5)		
$\angle(Z, a), (Y, c)$ (deg)	$\pm 30.247(14)$	$\pm 30.290(11)$		
$\angle(X, b)$ (deg)	0.00(8)	—		
(b)	$\text{NH}_4^{35}\text{ClO}_4$			
$ e^2qQ/h $ (kHz)	694.9(5)	$\sigma_0$ (PPM)	-917.5(7)	
$\eta$	0.7552(12)	$\Delta\sigma_X$ (PPM)	-1.4(12)	
		$\Delta\sigma_Y$ (PPM)	-15.3(8)	
		$\Delta\sigma_Z$ (PPM)	16.7(9)	
$\angle(Z, a), (X, c)$ (deg)	$\pm 16.58(3)$		$\pm 21(2)$	
$\angle(Y, b)$ (deg)	0.00(1)		0(2)	

of the two possible  $Z$  axes of nuclear quadrupole interaction and  $33^\circ$  away from the nearest possible  $Y$  axis (table 4(a)): a tentative assignment would put the molecular  $Z$  axis (which is the primary one) closest to the field. The field is also close to the twofold axis adopted by the molecule when rotation ceases, as revealed by neutron diffraction at 10 K [1].

The field acting on the  $\text{ClO}_4$  group amounts to  $0.588 \text{ V \AA}^{-1}$  and its cartesian direction is  $(0.475 \ 0 \ -0.880)$ . This direction is not obviously related to any bond or nuclear interaction, so no assignment is offered. We may note, however, that according to the refinement of [6], the centre of the four O atoms is displaced from the Cl position by as much as  $0.020(2) \text{ \AA}$  at 297 K, and the direction of this molecular dipole agrees (within experimental error) with that of the calculated field. The dipole has minimum electrostatic energy if the chlorine atom is charged positively with respect to the oxygens.

## 6. Deuteron resonance

At room temperature the spectrum of  $^2\text{H}$  is motionally narrowed by the rapid rotation of the ammonium groups, which averages out the anisotropic interactions. In the deuterated compound the powder linewidth is 0.73 kHz [4]. However, single-crystal  $b$ - and  $c$ -axis rotations (perpendicular to the field) reveal a complicated, angular-dependent structure in which several sharp features, possibly due to a liquid phase, are superimposed on and partly obscure a broader absorption straddling the  $\text{D}_2\text{O}$  frequency. The rotational period for the entire pattern is  $180^\circ$ . The broad spectrum, which has a minimum width of 0.4 kHz at the orientation  $\langle 001 \rangle$ , changes with orientation as if subject to bulk diamagnetism and residual shielding-anisotropy. We tentatively ascribe this spectrum to incomplete motional averaging of shielding anisotropy and dipolar interaction.

## 7. Conclusions

Our main findings are as follows.

- (i) The final results are those given in table 4, the estimation errors being low.
- (ii) The EFG tensors at the N and Cl sites are dissimilar, having different asymmetry parameters and different orientations. In both cases, however, the primary  $Z$  axis lies in the  $ac$  plane.
- (iii) Complete replacement of hydrogen by deuterium reduces the  $^{14}\text{N}$  quadrupole coupling constant by about 2%. The effect is small, as might be expected, but is easily measurable.
- (iv) At the Cl site, the anisotropic part of the chemical shielding tensor is approximately proportional to the EFG tensor.
- (v) Between room temperature and 150 K there is no sign of a phase transition affecting the  $^{14}\text{N}$  quadrupole coupling by more than a few percent. The broad maximum shown in figure 3(c) probably indicates no more than a continuous change in structure and dynamics, such as is responsible for the minimum in the lattice parameter  $b$  around 150 K [3].

### Acknowledgments

We are indebted to Dr A W Stevenson for the x-ray confirmation of the orientation of our lozenge and columnar form crystals, and to Dr S L Segel for his help in interpreting the temperature-dependent data.

### References

- [1] Choi C S, Prask H J and Prince E 1974 *J. Chem. Phys.* **61** 3523–9
- [2] Chakraborty T, Khatri S S and Verma A L 1986 *J. Chem. Phys.* **84** 7018–27
- [3] Prask H J, Choi C S, Chesser N J and Rosasco G J 1988 *J. Chem. Phys.* **88** 5106–22
- [4] Bastow T J, Brown R J C and Segel S L 1988 *J. Chem. Phys.* **89** 1203–4
- [5] Segel S L, Maxwell S, Heyding R D, Ingman P, Ylinen E and Punkkinen M 1988 *Solid State Commun.* **66** 1039–41
- [6] Choi C S and Prask H J 1976 *Acta Crystallogr. B* **32** 2919–20
- [7] Volkoff G M, Petch H E and Smellie D W L 1952 *Can. J. Phys.* **30** 270–88
- [8] Birge R T 1932 *Phys. Rev.* **40** 207–27
- [9] Wasylishen R E and Friedrich J O 1984 *J. Chem. Phys.* **80** 585–7
- [10] Volkoff G M 1953 *Can. J. Phys.* **31** 820–36